Tunable negative-tap photonic microwave filter based on a cladding-mode coupler and an optically injected laser of large detuning

Sze-Chun Chan,* Qing Liu, Zhu Wang, and Kin Seng Chiang

Department of Electronic Engineering, City University of Hong Kong, Hong Kong, China

**scchan@cityu.edu.hk*

Abstract: A tunable negative-tap photonic microwave filter using a cladding-mode coupler together with optical injection locking of large wavelength detuning is demonstrated. Continuous and precise tunability of the filter is realized by physically sliding a pair of bare fibers inside the cladding-mode coupler. Signal inversion for the negative tap is achieved by optical injection locking of a single-mode semiconductor laser. To couple light into and out of the cladding-mode coupler, a pair of matching long-period fiber gratings is employed. The large bandwidth of the gratings requires injection locking of an exceptionally large wavelength detuning that has never been demonstrated before. Experimentally, injection locking with wavelength detuning as large as 27 nm was achieved, which corresponded to locking the 36-th side mode. Microwave filtering with a free-spectral range tunable from 88.6 MHz to 1.57 GHz and a notch depth larger than 35 dB was obtained.

OCIS codes: (060.0060) Fiber optics and optical communications; (140.3520) Lasers, injection-locked; (070.6020) Continuous optical signal processing; (350.4010) Microwaves.

References and links

1. J. P. Yao, "Microwave photonics," J. Lightwave Technol. **27**, 314–335 (2009).
2. R. A. Minasian, "Photonic signal processing of microwave signals," IEEE Trans. Microwave Theory Tech. **54**, 832–846 (2006).
3. J. Capmany, B. O. Ortega, and D. Pastor, "A tutorial on microwave photonic filters," J. Lightwave Technol. **24**, 201–229 (2006).
4. S. Sales, J. Capmany, J. Marti, and D. Pastor, "Experimental demonstration of fiber-optic delay line filters with negative coefficients," Electron. Lett. **31**, 1095–1096 (1995).
5. J. Capmany, J. Mora, B. Ortega, and D. Pastor, "Microwave photonic filters using low-cost sources featuring tenability, reconfigurability and negative coefficients," Opt. Express **13**, 1412–1417 (2005), `http://www.opticsinfobase.org/oe/abstract.cfm?URI=oe-13-5-1412`.
6. T. Chen, X. K. Yi, T. Huang, and R. A. Minasian, "Multiple-bipolar-tap tunable spectrum sliced microwave photonic filter," Opt. Lett. **35**, 3934–3936 (2010).
7. F. Zeng, J. Wang, and J. P. Yao, "All-optical microwave bandpass filter with negative coefficients based on a phase modulator and linearly chirped fiber Bragg gratings," Opt. Lett. **30**, 2203–2205 (2005).
8. J. Wang, F. Zeng, and J. P. Yao, "All-optical microwave bandpass filter with negative coefficients based on PM-IM conversion," IEEE Photon. Technol. Lett. **17**, 2176–2178 (2005).
9. S. P. Li, K. S. Chiang, A. Gambling, Y. Liu, L. Zhang, and I. Bennion, "A novel tunable all-optical incoherent negative-tap fiber-optic transversal filter based on a DFB laser diode and fiber Bragg gratings," IEEE Photon. Technol. Lett. **12**, 1207–1209 (2000).

#142619 - $15.00 USD Received 15 Feb 2011; revised 24 May 2011; accepted 27 May 2011; published 7 Jun 2011

10. S. C. Chan, "Analysis of an optically injected semiconductor laser for microwave generation," IEEE J. Quantum Electron. **46**, 421–428 (2010).
11. D. Norton, S. Johns, C. Keefer, and R. Soref, "Tunable microwave filtering using high dispersion fiber time delays," IEEE Photon. Technol. Lett. **6**, 831–832 (1994).
12. E. H. W. Chan and R. A. Minasian, "Widely tunable, high-FSR, coherence-free microwave photonic notch filter," J. Lightwave Technol. **26**, 922–927 (2008).
13. S. Mansoori and A. Mitchell, "RF transversal filter using an AOTF," IEEE Photon. Technol. Lett. **16**, 879–881 (2004).
14. D. Pastor, J. Capmany, and B. Ortega, "Broad-band tunable microwave transversal notch filter based on tunable uniform fiber Bragg gratings as slicing filters," IEEE Photon. Technol. Lett. **13**, 726–728 (2001).
15. Z. Wang, K. S. Chiang, and Q. Liu, "All-fiber tunable microwave photonic filter based on a cladding-mode coupler," IEEE Photon. Technol. Lett. **22**, 1241–1243 (2010).
16. Z. Wang, K. S. Chiang, and Q. Liu, "Microwave photonic filter based on circulating a cladding mode in a fiber ring resonator," Opt. Lett. **35**, 769–771 (2010).
17. T. B. Simpson and J. M. Liu, "Phase and amplitude characteristics of nearly degenerate four-wave mixing in Fabry-Perot semiconductor lasers," J. Appl. Phys. **73**, 2587–2589 (1993).
18. S. C. Chan, S. K. Hwang, and J. M. Liu, "Period-one oscillation for photonic microwave transmission using an optically injected semiconductor laser," Opt. Express **15**, 14921–14935 (2007), http://www.opticsinfobase.org/oe/abstract.cfm?URI=oe-15-22-14921.
19. E. K. Lau, H. K. Sung, and M. C. Wu, "Frequency response enhancement of optical injection-locked lasers," IEEE J. Quantum Electron. **44**, 90–99 (2008).
20. J. M. Luo and M. Osinski, "Stable-locking bandwidth in sidemode injection locked semiconductor lasers," Electron. Lett. **27**, 1737–1739 (1991).
21. Y. Hong and K. A. Shore, "Locking characteristics of a side-mode injected semiconductor laser," IEEE J. Quantum Electron. **35**, 1713–1717 (1999).
22. Y. Hong, K. A. Shore, J. S. Lawrence, and D. M. Kane, "Wavelength switching by positively detuned side-mode injection in semiconductor lasers," Appl. Phys. Lett. **76**, 3170–3172 (2000).
23. S. P. Li, K. T. Chan, and C. Y. Lou, "Wavelength switching of picosecond pulses in a self-seeded Fabry-Perot semiconductor laser with external fiber Bragg grating cavities by optical injection," IEEE Photon. Technol. Lett. **10**, 1094–1096 (1998).
24. X. Wang and K. T. Chan, "Tunable all-optical incoherent bipolar delay-line filter using injection-locked Fabry-Perot laser and fiber Bragg gratings," Electron. Lett. **36**, 2001–2002 (2000).
25. C. L. Tseng, C. K. Liu, J. J. Jou, W. Y. Lin, C. W. Shih, S. C. Lin, S. L. Lee, and G. Keiser, "Bidirectional transmission using tunable fiber lasers and injection-locked Fabry-Perot laser diodes for WDM access networks," IEEE Photon. Technol. Lett. **20**, 794–796 (2008).
26. M. R. Uddin and Y. H. Won, "All-optical wavelength conversion by the modulation of self-locking state of single-mode FP-LD," IEEE Photon. Technol. Lett. **22**, 290–292 (2010).
27. Y. Liu, K. S. Chiang, Y. J. Rao, Z. L. Ran, and T. Zhu, "Light coupling between two parallel CO_2-laser written long-period fiber gratings," Opt. Express **15**, 17645–17651 (2007), http://www.opticsinfobase.org/abstract.cfm?URI=oe-15-26-17645
28. Y. Liu, H. W. Lee, K. S. Chiang, T. Zhu, and Y. J. Rao, "Glass structure changes in CO_2-laser writing of long-period fiber gratings in boron-doped single-mode fibers," J. Lightwave Technol. **27**, 857–863 (2009).
29. K. S. Chiang, F. Y. M. Chan, and M. N. Ng, "Analysis of two parallel long-period fiber gratings," J. Lightwave Technol. **22**, 1358–1366 (2004).

1. Introduction

Photonic microwave filters employ combinations of optical delay-lines for photonic processing of microwave signals. They possess unique characteristics of large bandwidth, high resolution, reconfigurability, and immunity to electromagnetic interference. Incorporation of wavelength division multiplexing enables low-noise performance due to mitigation of phase-induced intensity noise (PIIN). Photonic microwave filters have been investigated for a range of applications including antenna remoting in defense, channel selection in radioastromony, and signal processing in radio-over-fiber communication [1–3].

Realization of negative tap coefficients is essential to bandpass filters, according to fundamental signal processing theory. In order to avoid undesirable optical interference noise, several incoherent approaches have been reported based on differential detectors [4], electro-optical modulators with complementary arms [5, 6], and phase modulators [7, 8]. However, these approaches correspondingly involved electronic signal processing, special modulator designs, and

#142619 - $15.00 USD Received 15 Feb 2011; revised 24 May 2011; accepted 27 May 2011; published 7 Jun 2011

carefully matched dispersive devices. As a result, implementation of negative taps using injection locking of single-mode semiconductor lasers has remained an attractive alternative [9, 10]. Due to the mechanism of gain depletion, the free-running wavelength of an injected laser carries an inverted signal that is complementary to the injected signal. The regenerative signal from the locked laser has to be optically filtered out subsequently to eliminate PIIN. Nonetheless, the approach is a simple all-optical solution to realizing negative-tap photonic microwave filter.

Tunability of the photonic microwave filters has to be provided by adjustable delay mechanisms. A common approach employs a tunable optical source together with a dispersive element [11–14]. The accessible delay is limited by the tuning range of the source and the dispersion. Recently, a novel all-fiber tunable delay line has been realized [15,16]. It is based on using a cladding-mode coupler formed with two parallel bare fibers to physically adjust the length of the delay line, which enables continuous, precise, and wavelength-insensitive tuning of the delay time. The coupler requires only a pair of matching long-period fiber gratings (LPFGs) to launch the cladding mode at the input and convert it back to the core mode at the output.

In this work, a tunable negative-tap photonic microwave filter is investigated, where tunability is enabled by a cladding-mode coupler and signal inversion for the negative tap is achieved by optical injection locking. The LPFGs that are used in conjunction with the cladding-mode coupler not only provide mode coupling but also act as an optical filter to eliminate unwanted regenerative signal from the injected laser. The approach offers a compact, inexpensive, and continuously tunable configuration for negative-tap filtering. For demonstration, negative-tap filtering with a free-spectral range (FSR) tunable from 88.6 MHz to 1.57 GHz was obtained.

Because typical LPFGs have large resonance bandwidths of over 10 nm, the injection wavelength has to be detuned from the free-running wavelength of the laser by a large amount. The required detuning is much greater than the typical mode separation of semiconductor lasers, so that largely detuned side-mode injection locking has to be considered. Such injection is different from the nearly degenerate injection commonly investigated in injection locking dynamics [10,17–19], which concerns only one laser mode. Previous theoretical and experimental results indicate that side-mode injection locking is possible when the injection compensates the excess gain required by the side mode for lasing [20–22]. However, related applications with single-mode lasers usually involve detuning wavelengths that rarely go beyond a few nanometers or several laser mode separations [9, 23–26]. In our experiments, we demonstrate the photonic microwave filter using side-mode injection locking with wavelength detuning as large as 27 nm, which correspond to locking the 36-th side mode. The detuning is chosen for an optimal performance of the cladding-mode coupler.

Following this introduction, the experimental setup is presented in Section 2. Experimental results are reported in Section 3, which is followed by a conclusion in Section 4.

2. Principle of operation

The schematic of the experimental setup is shown in Fig. 1. A tunable laser (Agilent 8164B) emitting at λ_i was used as the master laser. The continuous-wave emission from the master laser was then modulated by an external amplitude modulator (Integrated Optical Component 2.5-Gbps Modulator) biased in the linear regime under an input RF signal of 11 dBm. The modulated light was amplified by an erbium-doped fiber amplifier (Amonics AEDFA-23-B-FA) to about 16 mW before being injected into the slave laser through a 50:50 fiber coupler (FC1). A polarization controller was adopted to match the polarization of the injection light to that of the slave laser modes.

The slave laser was a single-mode distributed feedback laser (Nortel LC111-18) that was temperature-stabilized by a thermoelectric cooler. It was biased at 56 mA that was above its threshold of 20 mA. When the injection was turned off, the free-running emission wavelength

#142619 - $15.00 USD Received 15 Feb 2011; revised 24 May 2011; accepted 27 May 2011; published 7 Jun 2011

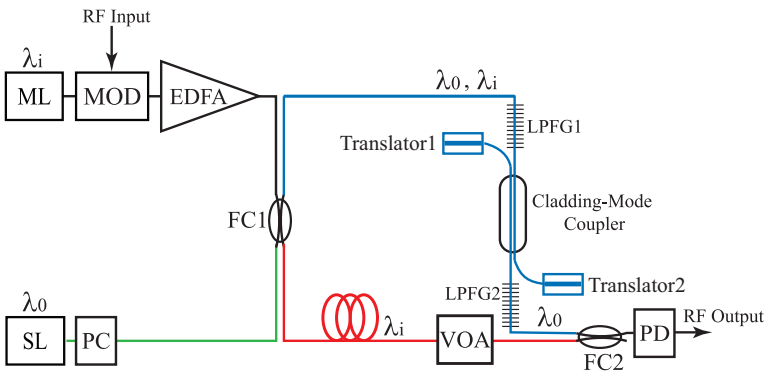

Fig. 1. Schematic of the tunable negative-tap photonic microwave filter. ML: master laser; SL: slave laser; MOD: amplitude modulator; EDFA: erbium-doped fiber amplifier; FC1, FC2: fiber couplers; PC: polarization control; LPFG1, LPFG2: long-period fiber gratings; PD: photodetector; VOA: variable optical attenuator. The red path transmits the non-inverted signal. The blue path transmits the inverted signal. FSR is determined by the time-delay difference that can be tuned at the cladding-mode coupler.

from the slave laser was λ_0 = 1548 nm at a power level of 0.5 mW. The output of the slave laser was then sent through the fiber coupler and optically filtered through a pair of LPFGs (LPFG1 and LPFG2) and a cladding-mode coupler. A second 50:50 fiber coupler (FC2) then combined the filtered output from the slave laser with a signal from the master laser. The resultant output was then converted into an output RF signal by a photodetector (New Focus 1014-IR).

The principle of operation of the photonic microwave filter is as follows. The input RF signal is modulated onto λ_i, which is injected into the slave laser through the green path in Fig. 1. By injection locking, the slave laser output contains both the free-running wavelength λ_0 and the regenerated wavelength λ_i. When the injection power increases, the emission power at λ_0 reduces while that at λ_i increases. Thus, an inverted RF signal is carried by λ_0 and a non-inverted RF signal is carried by λ_i, which are transmitted through the green path into the blue path. As light transmits through LPFG1, the inverted signal at λ_0 is coupled from the core mode to a cladding mode while leaving λ_i unaffected in the core mode. The cladding mode at λ_0 is switched to another fiber inside the cladding-mode coupler and coupled back to the core mode by LPFG2. On the other hand, in the red path, the non-inverted RF signal at λ_i from the master laser simply transmits through a fixed length of fiber. The photodetector receives both the inverted signal in the blue path at λ_0 from the slave laser and the non-inverted signal in the red path at λ_i from the master laser. Therefore, a negative-tap filter is realized with

$$\mathrm{FSR} = \frac{c}{n_g \Delta L_{\mathrm{eff}}}, \tag{1}$$

where c is the speed of light in vacuum, n_g is the group index, and ΔL_{eff} is the effective length difference obtained from subtracting the red path by the the sum of the blue path and twice the green path. The green path is counted twice because the signal has to be transmitted into and from the slave laser. As Fig. 1 shows, the FSR can be easily tuned by varying ΔL_{eff} through simply sliding the bare fibers inside the cladding-mode coupler with the two translators in the blue path. The notch depth of the filter can be maximized by matching the amplitude of the non-inverted signal to that of the inverted signal though fine-tuning the variable optical attenuator in the red path.

#142619 - $15.00 USD Received 15 Feb 2011; revised 24 May 2011; accepted 27 May 2011; published 7 Jun 2011

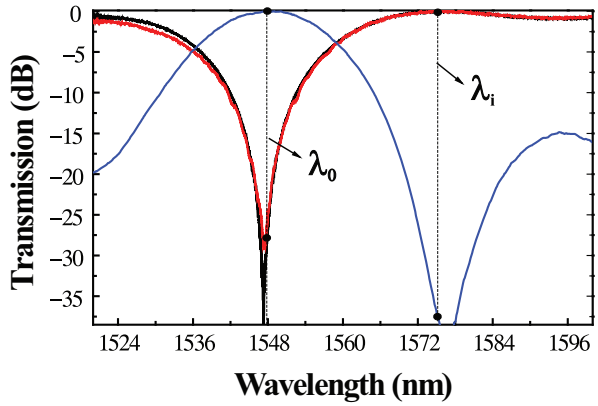

Fig. 2. Normalized transmission spectra (red and black) of the two LPFGs and the overall transmission spectrum (blue), which shows that λ_i remains in the core mode while λ_0 is coupled to the cladding mode.

3. Experimental results

3.1. Cladding-mode coupling

The LPFGs were written in a B-Ge co-doped fiber (Fibercore PS1250/1500) using a CO_2 laser [27, 28]. The grating was inscribed in the core for axial symmetry that allowed polarization-independent operation [27, 28]. The pitch and the number of periods of the LPFGs were 334.5 μm and 100, respectively. The gratings provided strong coupling between the core mode and the LP_{08} cladding mode at the free-running wavelength of the slave laser λ_0 = 1548 nm. The normalized transmission spectra of the two LPFGs are shown as the red and black curves in Fig. 2, which reveal clear resonances of more than 28.0 dB at λ_0. To avoid coupling the core mode into the cladding mode at λ_i, λ_i = 1575 nm was chosen for maximal core-mode transmission. Thus, λ_i always remained in the core mode while λ_0 was coupled to the cladding mode.

The cladding-mode coupler was constructed with a pair of parallel, touching bare fibers placed in a groove made of coated low-index silicone polydimethylsiloxane (PDMS) [15] to allow strong evanescent-field coupling between the cladding modes of the fibers [29]. The time delay of the blue path can be easily tuned by sliding the fibers along the groove with the help of the translators. The length of the groove was 57.5 mm. The normalized transmission spectrum measured at the output of LPFG2 in relation to the input of LPFG1 through the cladding-mode coupler is shown as the blue curve in Fig. 2, where it is observed that λ_0 is transmitted through the LPFGs and the coupler, whereas λ_i is blocked with a contrast ratio of 37.5 dB. Such a high contrast ratio rendered interference with λ_i in the red path negligible, thus mitigating the undesirable PIIN at the photodetector.

3.2. Optical injection locking

The large bandwidth of LPFGs, as shown in Fig. 2, required a separation of λ_0 and λ_i beyond typical laser mode separations of semiconductor lasers. Side-mode injection locking of large detuning was therefore employed. The injection power was controlled by the amplitude modulator. The optical spectra of the slave laser emission when the injection power was off and on are shown as the red and black curves in Fig. 3, respectively. The resolution bandwidth of the optical spectrum analyzer was 0.6 nm.

#142619 - $15.00 USD Received 15 Feb 2011; revised 24 May 2011; accepted 27 May 2011; published 7 Jun 2011

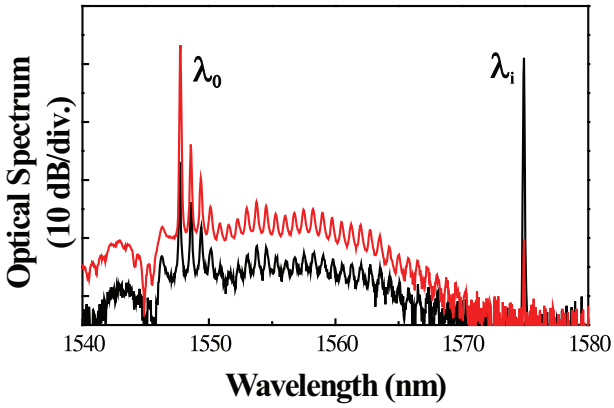

Fig. 3. Optical spectra of the slave laser emission when the injection power was off (red) and on (black).

When the injection power was off, a strong peak at λ_0 was observed together with residual emissions at the side modes. The side-mode suppression ratio (SMSR) was about 18 dB with a mode separation of about 0.75 nm. A very weak regenerative peak at λ_i was merely caused by leakage from the amplitude modulator. When the injection power was increased to its maximum, the slave laser was progressively locked by λ_i. The corresponding spectrum in Fig. 3 shows that the power level at λ_i was increased by 31 dB. Because of the gain depletion effect, λ_0 was drastically weakened by about 20 dB. Therefore, by injection locking, signal inversion at λ_0 was successfully realized. Other side modes were suppressed by the injection simultaneously.

It is worth noting that the wavelength detuning was as large as $\lambda_i - \lambda_0 = 27$ nm. The injection locked the 36-th side mode according to Fig. 3. To our best knowledge, the detuning demonstrated here was the largest among related previous experiments for wavelength conversion in single-mode lasers [26], which can be attributed to the modest SMSR of our laser. In addition, some previous experiments suggested that locking favors injection with λ_i being shorter than λ_0 [21]. We conducted locking experiments at $\lambda_i = 1521$ nm for $\lambda_i - \lambda_0 = -27$ nm and found that the required injection power for locking was increased by about 10 dB. The substantial increment of the required power was due to the asymmetric gain spectrum of our laser, where wavelengths shorter than λ_0 generally experienced less gain than those longer than λ_0 [20]. Therefore, λ_i was kept at 1575 nm in our filtering experiments.

3.3. Tunable filter response

The normalized output of the negative-tap filter was measured as the input RF frequency was varied. The results for different FSRs using different length differences ΔL_{eff} are shown in Fig. 4, where the dots are measurement data from an electrical spectrum analyzer and the curves are the best-fit sinusoidal functions. There is always a notch at the zero frequency that is characteristic of a negative-tap filter. By adjusting the variable optical attenuator in Fig. 1 to about 25 dB, the received signal amplitudes from the red and blue paths were matched at the photodetector. A resultant notch depth larger than 35 dB was achieved, as limited by the noise floor of our detection electronics.

For illustration, Fig. 4(a) shows the filter responses with FSRs from 88.6 MHz to 97.6 MHz as the effective length difference ΔL_{eff} was varied from 233 cm to 212 cm. Precise tuning was achieved by adjusting the mechanical translators attached to the cladding-mode coupler. Also,

#142619 - $15.00 USD Received 15 Feb 2011; revised 24 May 2011; accepted 27 May 2011; published 7 Jun 2011

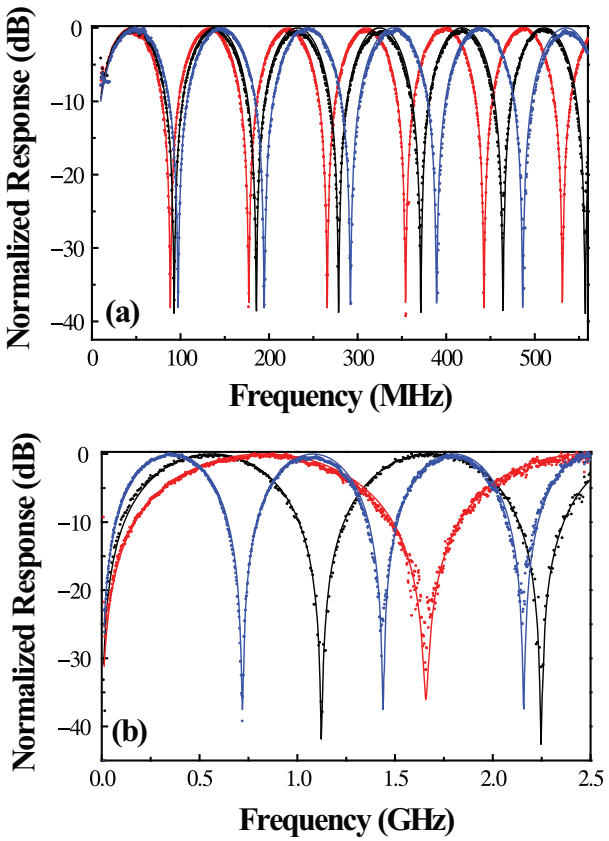

Fig. 4. Measured (dots) and calculated (curves) frequency responses of the microwave photonic filter for FSR = (a) 97.6 MHz, 93.3 MHz, and 88.6 MHz; and (b) 1.57 GHz, 1.13 GHz, and 0.719 GHz.

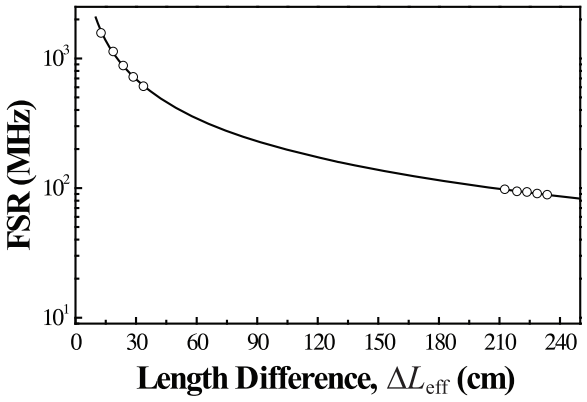

Fig. 5. Dependence of the FSR on the length difference ΔL_{eff}.

#142619 - $15.00 USD Received 15 Feb 2011; revised 24 May 2011; accepted 27 May 2011; published 7 Jun 2011

high-frequency operation can be realized by reducing ΔL_{eff}. Figure 4(b) shows an FSR tunable from 0.719 GHz to 1.57 GHz. The FSR can be increased by reducing ΔL_{eff} until being limited by the optical modulation bandwidth of the laser, which is typically on the order of 10 GHz. Tuning of the negative-tap filter is summarized in Fig. 5, where the measured data in circles are fit to the curve for group index n_g = 1.45. Fine-tuning of the FSR is allowed by precisely adjusting the translators. From Eq. (1), even with a modest mechanical precision of 0.2 mm in our setup, the precision of FSR is better than 0.1% when operated at FSR = 1 GHz. The tuning range of ΔL_{eff} is limited by the lengths of the bare fibers that can be maneuvered, which is typically up to a few tens of centimeters. Such precise and wide tunability offered by the cladding-mode coupler is difficult to achieve with conventional delay-tuning approaches.

It is possible to extend the current configuration to accommodate more taps. A simple approach to realizing two negative taps is to tap out some light from the first delay path with a fiber coupler (at a position before LPFG1 in Fig. 1), transmit the tapped signal through a second delay path that consists of another set of LPFG pair and cladding-mode coupler, and combine the output signal from the second delay path with the signals from the original paths. To avoid PIIN, a polarization controller should be inserted in the second path to ensure orthogonal polarization states between the two negative taps. A variable optical attenuator can also be inserted in the second delay path to control the magnitude of the tap coefficient. A general approach to realizing *N* negative taps is to employ *N* slave lasers of different free-running wavelengths locked by the same master laser. The inverted signals at the *N* wavelengths are extracted, respectively, by *N* stages of LPFG pair and cladding-mode coupler, which are connected in series through the idle output ports of the cladding-mode couplers. The LPFG pair at each stage is designed to operate only at the assigned signal wavelength. The output signals from the *N* stages and the non-inverted signal from the master laser are finally combined to produce the filter output. The tap coefficients can be varied independently by adjusting the polarization controllers that control the injection locking of the slave lasers. The maximum number of negative taps that can be achieved is mainly limited by the bandwidths of the LPFGs and the number of slave lasers that can be locked effectively with a single master laser.

4. Conclusion

In summary, a tunable negative-tap photonic microwave filter is proposed, which employs a largely detuned injection-locked laser for signal inversion and a cladding-mode coupler for compact, precise, and continuous tuning. The use of a pair of LPFGs in conjunction with the cladding-mode coupler enables both optical filtering and delay tuning. An experimental filter was demonstrated with an FSR tunable from 88.6 MHz to 1.57 GHz with a notch depth larger than 35 dB. Optical injection locking with wavelength detuning as large as 27 nm was achieved. The approach is readily extended to multiple-tap filters, as multiple path lengths can be adjusted precisely using cladding-mode couplers.

Acknowledgments

The work described in this paper was fully supported by two grants from City University of Hong Kong [Project Nos. CityU 7002444 and CityU 7002448].

#142619 - $15.00 USD Received 15 Feb 2011; revised 24 May 2011; accepted 27 May 2011; published 7 Jun 2011